Redox Biology 56 (2022) 102456

Contents lists available at ScienceDirect

Redox Biology

journal homepage: www.elsevier.com/locate/redox

Role of redox-sensitive catalytic interaction with ADAM10 in mutant-selective extracellular shedding of prion protein

Yejin Shin [a,b], Kang-Sug Jo [a,b], Minseok Shin [a,b], Duri Lee [a,b], Hyejin Yeo [a,b], Youngsup Song [a,b,c], Sang-Wook Kang [a,b,c,*]

[a] Department of Biomedical Sciences, University of Ulsan College of Medicine, Seoul, Republic of Korea
[b] Asan Medical Institute of Convergence Science and Technology, Asan Medical Center, Seoul, Republic of Korea
[c] Asan Institute of Life Sciences, Asan Medical Center, Seoul, Republic of Korea

ARTICLE INFO

Keywords:
Protein quality control
Protein shedding
Prion protein
ADAM10
Redox

ABSTRACT

Misfolded glycosylphosphatidylinositol-anchored prion protein (PrP) is primarily degraded in lysosomes but is often rapidly removed from the cell surface before endocytosis in a preemptive manner. However, this mechanism is poorly understood. In this study, we discovered a disease-causing prion mutation (Q212P) that exceptionally promoted the extracellular release of PrP. Spatiotemporal analyses combined with genome editing identified the role of sheddase ADAM10 in Q212P shedding from the cell surface. ADAM10 was observed to catalytically interacts with Q212P but non-catalytically with wild-type PrP (wtPrP). This intrinsic difference in the interaction of ADAM10 between Q212P and wtPrP allowed Q212P to selectively access the sheddase activity of ADAM10 in a redox-sensitive manner. In addition, redox perturbation instigated the latent misfolding propensity of Q212P and disrupted the catalytic interaction between PrP and ADAM10, resulting in the accumulation of misfolded PrP on the cell surface. Upon recovery, active ADAM10 was able to reversibly release the surface Q212P. However, it might prove detrimental if unregulated resulting in unexpected proteotoxicity. This study provides a molecular basis of the mutant-selective shedding of PrP by demonstrating the catalytic interaction of ADAM10 with Q212P.

1. Introduction

Secretory and membrane proteins newly synthesized in the endoplasmic reticulum (ER) undergo folding, modifications, and a complex assembly during transit through the secretory pathway. This enables the proteins to acquire unique three-dimensional structures for efficient functioning [1]. These processes require a sophisticated collaboration of various molecular chaperones and are prone to perturbation by mutations, translational errors, or different environmental stresses [2]. In general, these perturbations restrict many newly synthesized proteins from folding properly and therefore, such proteins are efficiently removed by a timely activation of quality control (QC) mechanisms [3,4]. However, some misfolded proteins may accumulate in secretory organelles or on the cell surface, leading to risks of proteotoxicity [5,6].

ER-associated degradation (ERAD) is the most extensively studied and conceptualized QC mechanism in the stressed ER, in which thousands of misfolded substrates with varying biophysical parameters are recognized by adaptors in the ER lumen, delivered to the cytosolic side, extracted from the ER, and degraded in the proteasome. The first two steps are critical and therefore, tightly controlled in a substrate-specific manner in the ER lumen, while the next two occur in the cytosol and are shared by almost all substrates [4,7]. Owing to this, at present, the major interest lies in elucidating the factors or mechanisms that discriminate potential ERAD substrates expected to be misfolded from a pool of newly synthesized proteins in the folding process. For example, misfolding of glycoproteins identified as the most extensively studied group of ERAD substrates is mediated by aberrant glycan modifications and is recognized by ER-resident lectins [8,9]. However, not all misfolded proteins synthesized in the ER are degraded by ERAD. One such typical ERAD-resistant misfolding-prone protein is the prion protein (PrP) synthesized in a form covalently attached to the luminal side of the ER membrane by a glycosylphosphatidylinositol (GPI)-anchor [10].

PrP is a mysterious protein for which the conformational conversion from its native cellular form (PrP^{C}) to its pathological isoform (PrP^{SC})

* Corresponding author. Department of Biomedical Sciences, University of Ulsan College of Medicine, 88, Olympic-ro 43gil, Songpa-gu, Seoul, 05505, Republic of Korea.
E-mail address: swkang@amc.seoul.kr (S.-W. Kang).

https://doi.org/10.1016/j.redox.2022.102456
Received 3 August 2022; Received in revised form 21 August 2022; Accepted 22 August 2022

directly correlates with the pathogenesis of fatal neurodegenerative disorders [11]. More than 30 variants in the human *PrP* have been identified as causes of prion diseases characterized with diverse heterogeneous phenotypes [12,13]. Notably, these mutations often act during the conversion of PrP^C and perturb its trafficking or processing, therefore, resulting in the accumulation of misfolded PrP in intracellular compartments during passage through the secretory pathway [14]. Misfolded PrP accumulation may occurs due to inefficient clearance of conformationally problematic PrP mutants. This can be resolved by various QC mechanisms that are mechanistically different from ERAD and are rapidly activated in response to ER stress [15].

For example, preemptive QC (pQC) aborts the production of difficult-to-fold proteins, including PrP, at the step of protein translocation across the ER membrane [16]. In one of our recent studies, we have revealed that pQC is utilized for mutant-selective topologic conversion (MSTC) of PrP, which selectively removes the membrane-anchored PrP isoform (ctmPrP) and alleviates PrP proteotoxicity [17]. In addition, rapid ER stress-induced export (RESET) rapidly exports ERAD-resistant misfolded PrP from the stressed ER [18]. This exported PrP forms a complex with ER-derived chaperones and cargo receptors, is escorted through the secretory pathway, and is transiently expressed on the cell surface before being subjected to lysosomal degradation [19]. As such, both pQC and RESET are undoubtedly beneficial to reduce substrate burden and restore the folding capacity in stressed ER.

More recently, we found that the endocytosis of PrP mutants defective in the disulfide bridge, a well-characterized RESET substrate, is inhibited at the cell surface as a result of the removal of the unpaired free-thiol group through the plasma membrane QC (pmQC) mechanism [20]. pQC and pmQC act by reducing the burden of misfolded PrP entering the ER and lysosome, respectively. pQC is broadly utilized by the cells for many substrates in a signal sequence-dependent manner, whereas pmQC has a limited substrate range owing to its activation mediated in a conformation-dependent manner.

A disintegrin and metalloproteinase 10 (ADAM10), a major sheddase along with its close relative ADAM17, has been identified as a potential modulator of the pmQC for PrP [21,22]. ADAM10/17 are membrane-integrated proteins and ubiquitously expressed in mammalian cells. Thses proteins are able to function as molecular scissors and proteolytically cleave the extracellular regions or ectodomains of at least 40 integral membrane proteins playing important roles in cell adhesion, proliferation, differentiation, migration, immunity, and receptor-ligand signaling [23,24]. PrP is the first GPI-anchored protein identified as a common substrate for ADAM10/17 [25]. Of these, ADAM10 has been reported to cleave the site in close proximity to the GPI-anchor linked to the C-terminus of surface PrP between the amino acid positions, Gly^{228} and Arg^{229}, resulting in the release of anchorless PrP into the extracellular space [26]. Nevertheless, the processes regulating the extracellular release of anchorless PrP mediated by ADAM10/17 remain poorly defined.

In the present study, we found a naturally occurring pathogenic PrP mutant (Q212P) processed by pmQC. Spatiotemporal analysis of PrP expression, trafficking, and processing, combined with genome editing, identified ADAM10 as a pmQC regulator that triggered Q212P shedding from the cell surface. This study unraveled the molecular basis of this triage reaction that occurred at the cell surface in response to the environmental redox perturbations. This study also provided an insight into the ADAM10-mediated Q212P shedding as a peripheral QC to protect cells from the surface overload of misfolded PrP.

2. Materials and Methods

2.1. Antibodies and reagents

The following antibodies were used in this study: antisera for TRAPα, Sec61β, GFP, and RFP were as described previously [27–29]. Purchased antibodies included anti-FLAG M1 antibody (Merck, SF3040), anti-ADAM10 (Merck, AB19026), anti-ADAM17 (Abcam, ab2051), anti-GAPDH (Santa Cruz, SC-20357), anti-HA high affinity (Merck, 11867431001), anti-CD230 (prion) clone 3F4 (BioLegend, 800,307) and HRP-conjugated streptavidin (ThermoFisher, N100). The FLAG-conjugated GFP nanobody (GFP-Nb) was obtained as a gift from Ramanujan S. Hegde, MRC, UK [19].

Endo H, PNGase F, and all enzymes used for cloning were obtained from New England Biolabs. MG132, DTT, cycloheximide, thapsigargin and all chemicals used for the biochemical procedures in this study were purchased from Merck. Monensin and bafilomycin-A1 were purchased from MedChemExpress.

2.2. Cell culture analyses

Flp-In T-REx 293 cells were purchased from Invitrogen (R78007) and grown in Dulbecco's Modified Eagle's Medium (DMEM) supplemented with 10% fetal calf serum and incubated in 5% CO_2 at 37 °C. To establish CRISPR/Cas9 cell lines, Flp-In T-REx 293 cells were modified by the stable integration of the *Cas9* gene (cloned in pcDNA3), which promotes genome editing. Ten Flp-In T-REx 293-Cas9 cell lines were established by the clonal isolation of G418-resistant cells by serial dilution in 96 well plates, and their Cas9 activities were verified by T7E1 assay and immunoblotting. Isogenic cell lines with an inducible expression of stably integrated wild-type or mutant PrPs were generated according to the manufacturer's directions (Invitrogen) following transfection of plasmid constructs with Lipofectamine 2000 (Invitrogen). In this system, PrP expression was controlled by the CMV promoter activated by doxycycline (Dox) (10 ng/ml) for 16 h unless otherwise indicated. To establish an ADAM10-deficient cell line (ΔADAM10), the Flp-In T-REx 293-Cas9 cell line was transfected with a mixture of three ADAM10 and ADAM17 gRNA constructs as described (see "Molecular biology" section) for 24 h and incubated in the presence of puromycin (2 μg/mL) for an additional 48 h. Viable cells were maintained in culture media containing puromycin (0.5 μg/mL).

Subcellular localizations of PrPs were analyzed by directly visualizing the fluorescence in cells cotransfected with PrP fused with RFP and GFP as previously described [17,20], and images were obtained using a confocal microscope (Zeiss LSM880 with Airyscan; Carl Zeiss Microimaging) using the manufacturer's image acquisition software, ZEN 2.3 (black edition). Colony forming assays were performed using a previously published procedure with minor modifications [30]. Briefly, 100 cells per well were plated on 6-well dishes and cultured in DMEM supplemented with Dox for three weeks. Viable cell colonies were fixed and counterstained with 0.5% crystal violet in 6% glutaraldehyde, and visualized via GelCount™ (Oxford Optronix; Abington, UK) using the manufacturer's image acquisition software.

2.3. Molecular biology

The PrP coding region (GeneBank accession number: M13899) was PCR-amplified from the first-strand cDNA synthesized from HeLa cells and cloned into the HindIII and *Xho*I sites of the pcDNA5-FRT/TO vector (Invitrogen). All mutant constructs used in this study were engineered by conventional site-directed mutagenesis using Phusion high-fidelity DNA polymerase (New England BioLabs). Fluorescent protein (FP) fusion constructs were created by the insertion of GFP or RFP genes into the unique *Bsu*36I site within the N-terminal coding region of wtPrP and mutant PrP. ADAM10 constructs were created by the insertion of human cDNA encoding ADAM10 (GeneBank accession number: AF009615) into HindIII and *Xho*I sites of homemade pcDNA5-FRT/TO-HA vector. A mutant ADAM10 (AXXA) construct was constructed in the same manner as the PrP mutants.

ADAM10 depletion was implemented with the CRISPR/Cas9 genome editing. Two sets of scrambled gRNA sequences specifically targeting ADAM10 (ADAM10 gRNA #1, 5′-CCCATAAATACG GTCCTCAG-3'; ADAM10 gRNA #2, 5′-GAAGGATTCATCCAGACTCG-3'; ADAM10 gRNA

#3, 5′-TTTCAACCTACGAATGAAGA-3′) and ADAM17 (ADAM17 gRNA #1, 5′-AA TCAGAATCAACACAGATG-3’; ADAM17 gRNA #2, 5′-GAACACGTGTAAATTATTGG-3’; ADAM17 gRNA #3, 5′-TGGTGAAAAGCACTACAACA-3′) were selected based on the on-/off-target score given in CRISPick (https://portals.broadinstitute.org/gppx/crispick/public) and directly inserted into the *Bsm*BI sites of the lentiGuide-Puro vector [31], a gift from Feng Zhang (Addgene plasmid # 52,963). All constructs were confirmed by DNA sequencing (Cosmogenetech; Seoul, South Korea).

2.4. Biochemistry

Pulse-chase experiments were performed to determine PrP synthesis and turnover rates. PrP expression was induced by Dox (10 ng/ml) for 16 h before pulse-labeling. Cells were starved with serum-free and methionine/cysteine-free media for 30 min and pulse-labeled with a *trans*-labeling mixture ([^{35}S]-methionine/cysteine; PerkinElmer) for an additional 30 min. The spent medium was replaced with fresh growth medium, and the pulse-labeled cells were solubilized in buffer K (1% SDS, 100 mM Tris-HCl, pH 7.5) at the indicated time points and diluted to 10-folds with IPT buffer (1% Triton X-100, 50 mM HEPES, pH 7.5, 150 mM NaCl). PrP was captured by PrP-specific 3F4 antibody or anti-RFP for 90 min and recovered from cell lysates by protein G-conjugated magnetic beads (GE Healthcare Life Sciences) for an additional 90 min. The beads were washed five times with 1 mL of IPT buffer to remove nonspecific binding and resuspended in 30 μl of 1.5X SDS-PAGE sample buffer. Lysosome-restricted free RFP generation was assessed by monitoring the level of free RFP produced from newly synthesized intact PrP-RFP during the chase as previously described [20]. For immunoprecipitation (IP) of PrP-RFP in the extracellular space, cell culture media was collected, passed through the 0.45 μm syringe filter, and denatured by adding 0.1 volume of buffer K. The CM was incubated with an RFP-specific antibody and protein A-agarose beads for 90 min. The beads were washed five times with 1 ml of IPT buffer and resuspended in 30 μl of 1.5X SDS-PAGE sample buffer. In some experiments (Fig. 6), the CM was further analyzed by sequential centrifugation. The CM containing PrP-RFP was subjected to centrifugation at 300×*g* for 10 min. The supernatant was collected and further separated in a stepwise manner at 2000×*g* to 200,000×*g* for 20 min up to 1 h as described in Fig. 6C. The PrP-RFP was enriched in the supernatant or pellet from each centrifugation and detected by immunoblotting with an RFP-specific antibody.

For a stable isolation of PrP complexes expressed on the cell surface, surface-restricted labeling using GFP-Nb was performed as previously described [19] with minor modification. Briefly, PrPs-GFP were induced by the treatment with Dox (10 ng/ml) for 24 h, and these complexes were covalently linked with their interacting partners using 2 mM of DSP (ThermoFisher, 22,585) for 30 min at room temperature (RT). Following quenching with 20 mM of Tris (pH 7.5) for 15 min at RT, surface PrPs-GFP were selectively labeled with 100 nM FLAG-conjugated GFP-Nb prepared in 1X PBS supplemented with 10% FBS for 30 min at 4 °C. The labeled cells were solubilized in lysis buffer (1% CHAPS, 50 mM HEPES, 150 mM NaCl, 2 mM $MgCl_2$) for 10 min on ice and centrifuged at 16,000×*g* for 10 min to remove cell debris. The supernatant was further incubated with anti-FLAG M2 magnetic beads (Merck M8823) for 3 h at 4 °C. The beads were washed six times with lysis buffer, and the PrP-interacting partners crosslinked with surface PrP-GFP were eluted by the incubation with 30 μL of lysis buffer containing FLAG peptide (1 mg/mL) for 30 min at RT.

In all experiments involving IP, 10 μL of eluents were separated on gels and analyzed by autoradiography or immunoblotting with appropriate antibodies.

2.4.1. Miscellaneous

Comparative analyses of biochemical properties including glycosidase sensitivity, detergent solubility, trypsin sensitivity, and sucrose gradient centrifugation were performed as previously described [10,14,16,17]. In protein analysis experiments, the cells were fully solubilized in buffer K, boiled, and separated by SDS-PAGE using 10 or 12% Tris-tricine gels. The experimental conditions for each experiment have been described in individual figure legends.

2.5. Quantitation and statistical analysis

Average band intensities of immunoblotting were measured directly by Image Studio (LI-COR, Inc.), and those of ^{35}S incorporation into the newly synthesized proteins were inverted to black-and-white for clarity and measured by Image J (NIH) software. The calculations and protein expressions have been described in individual figure legends. The data has been presented as the mean ± standard deviation (S.D.) of more than three independent replicates. *n* represents the number of independent experiments. Statistical differences were analyzed using Student’s *t*-test, and their significance was expressed with *p*-values as follows; $*p < 0.05$, $**p < 0.005$, $***p < 0.001$.

3. Results

3.1. Q212P mutation promotes PrP trafficking and processing

This study was motivated by the discovery of a disease-causing PrP mutant (Q212P) showing a unique pattern of PrP subpopulations. Most notably, in contrast to wtPrP synthesized in four different forms corresponding to non-, mono-, di-, and fully glycosylated forms, Q212P was synthesized in two major forms, i.e., di- and fully-glycosylated forms (Fig. 1A). Of these two forms, the fully-glycosylated form modified by complex glycan while passing through post-ER compartments during the secretory pathway (i.e., as it is sensitive to PNGase F but resistant to Endo H) was selectively augmented by ~ 1.6-fold as a result of Q212P mutation (Fig. 1A, see also Fig. S1A). This pattern is not generally observed in pathogenic PrP mutants [14,32], as shown by the H187R mutant, which did not synthesize the fully glycosylated form (Fig. S1A). Nevertheless, the general pattern in subcellular localization of PrP was unchanged by the Q212P mutation, as visualized by the complete overlap of Q212P-RFP and wtPrP-GFP at the cell surface and intracellular compartments (Fig. S1B). In contrast, the surface localization of PrP was selectively inhibited by Q212P mutation through repressed de novo protein synthesis using cycloheximide (CHX), suggesting a possible role of Q212P mutation in promoting the clearance of surface PrP (Fig. 1B).

To explore this idea, we investigated the impact of the Q212P mutation on PrP synthesis and turnover using pulse-chase analysis. In this experiment, inducible expression of stably integrated untagged PrP allowed us to efficiently discriminate the small differences in sizes of folding intermediates transiently synthesized in transit through the secretory compartments. Consistent with the result of immunoblotting (Fig. 1A), wtPrP was newly synthesized in non-, mono-, and di-glycosylated forms in pulse-labeled cells, whereas the Q212P mutant was synthesized predominantly in a di-glycosylated form without detectable amounts of the other forms (Fig. 1C). During the chase, the di-glycosylated forms of both wtPrP and Q212P were trimmed with glucosidases in the ER within 30 min and further modified with complex glycans in the Golgi apparatus within 1 h. In contrast, mono-glycosylated wtPrP remained unmodified further in the ER until 4 h after the chase. Despite the similarity in the rate of post-ER trafficking, the fully glycosylated PrP was produced at a higher level in Q212P cells than in wtPrP cells. This could be attributed to the fact that the post-ER trafficking was allowed only for the di-glycosylated form initially synthesized in pulse-labeled cells, noting that a higher level of di-glycosylated PrP was newly synthesized in pulse-labeled Q212P cells (Fig. S1C). Thus, an accelerated PrP maturation mediated by the Q212P mutation might be a plausible explanation for the observed increase in fully glycosylated Q212P.

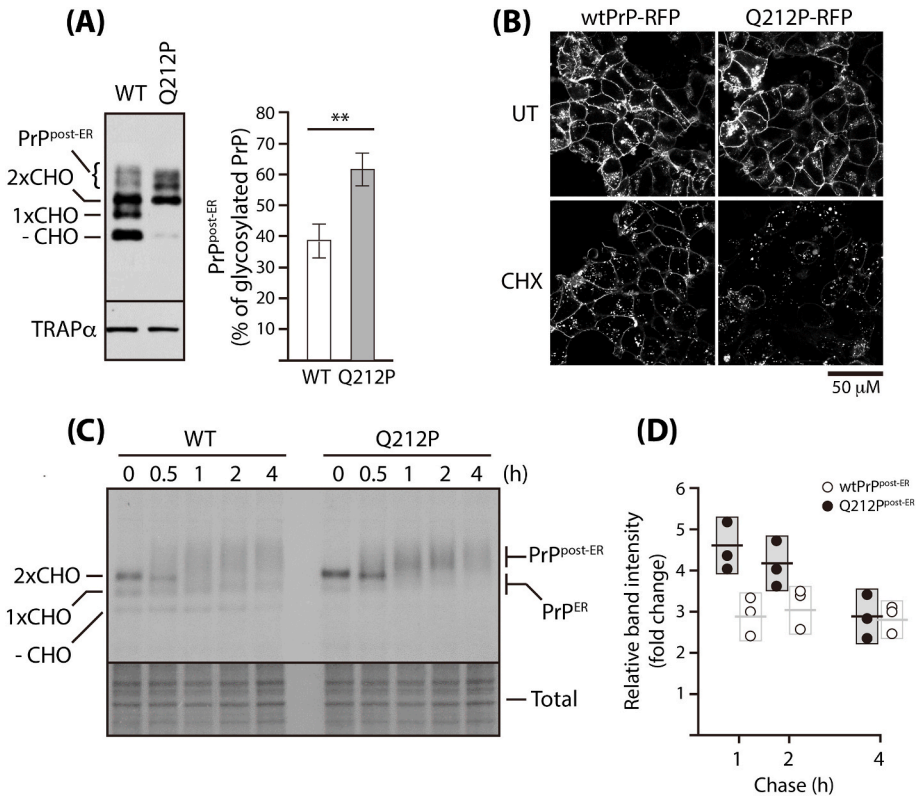

Fig. 1. Spatiotemporal analyses of PrP expression
(A) The effect of Q212P mutation on general patterns of PrP subpopulations accumulated in cells was analyzed by immunoblotting. Flp-In 293 T-Rex cells expressing untagged wild-type and disease-causing PrP mutant (i.e., Q212P) were fully solubilized and subjected to immunoblotting with a PrP-specific 3F4 antibody (1:20,000 dilution). Equal loading was confirmed by blotting with an anti-TRAPα antibody (left panel). Data were plotted as the percentage of fully glycosylated mature forms out of total glycosylated forms ($n = 4$; $p = 0.003$) (right panel). Note, –CHO: unglycosylated form, 1XCHO: monoglycosylated form, 2XCHO: doubly glycosylated form, $PrP^{post-ER}$: fully glycosylated mature form.
(B) The effect of Q212P mutation on the turnover of surface PrP was analyzed by the CHX-chase. Cells were co-transfected with constructs expressing wtPrP-GFP (left panel) and Q212P-RFP (right panel) and incubated for 18 h with Dox (10 ng/mL) to induce fluorogenic PrP expressions. Following further incubation for 1 h in the presence and absence of CHX (100 μg/mL), GFP and RFP fluorescence were directly visualized using confocal microscopy. Scale bar: 50 μm
(C) The effect of Q212P mutation on the metabolism and processing of PrP was assessed by pulse-chase experiments. Following expressions of stably integrated untagged wtPrP and Q212P induced by Dox, cells were pulse-labeled with [^{35}S]-methionine for 30 min and chased for indicated time before harvesting. Cells were fully solubilized in buffer K and subjected to immunoprecipitation with a 3F4 antibody (1:1000 dilution). Note, PrP^{ER}: mono- and di-glycosylated PrP in the ER, $PrP^{post-ER}$: fully matured PrP undergoing complex glycan modification, Total: total proteins newly synthesized and labeled with [^{35}S]-methionine in pulse-labeled cells.
(D) The band intensities of fully glycosylated PrP ($PrP^{post-ER}$) level synthesized at indicated time points during the chase in (C) were measured, quantified, and expressed as fold changes relative to the level initially synthesized during the pulse. The small horizontal bars represent the means of the three independent experiments.

3.2. Q212P mutation triggers the extracellular release of PrP

In our pulse-chase analyses, we noticed that fully glycosylated PrP was decreased selectively in Q212P cells by ~30% between 2 h and 4 h after the chase (Fig. 1C and D). Given the fact that lysosomes are the primary sites for the clearance and recycling of PrP, the logical explanation for the decrease in surface Q212P may be attributed to inhibitory endocytosis [18]. To investigate this idea, we employed a well-validated method [20] that has been previously used to determine the differential rate in lysosomal deliveries of wtPrP and mutant PrP inserted by RFP resistant to lysosomal acidic proteases. We reasoned that, by monitoring the level of free RFP in cells expressing RFP-inserted Q212P, we could verify the impact of the Q212P mutation on proteolytic endocytosis of PrP (Fig. 2A). A combination of this assay with pulse-chase experiments revealed that RFP insertion did not perturb the general pattern of PrP synthesis and turnover; the newly synthesized wtPrP-RFP was fully glycosylated within 1 h after the chase and then endocytosed and processed into free RFP (Fig. S2A). The fully glycosylated PrP was expressed on the cell surface within 1 h after the chase, as deduced through its complete digestion by exogenously added trypsin (Fig. 2B). In contrast, free RFP was protected by trypsin and increased progressively up to 4 h after the chase; however, its generation was suppressed by an inhibitor of lysosomal acidic proteases, bafilomycin A1 (BAF-A1) (Fig. 2C, see also Fig. S2B). Accelerated proteolytic endocytosis did not appear to be the sole reason for the reduction in surface Q212P owing to the unchanged level and rate of free RFP generation post its mutation (Fig, 2B, see also Fig. S2A). This might be a reasonable explanation for the increase in accumulated Q212P accumulated at the cell surface (Fig. 1A). Therefore, we aimed to identify an additional mechanism by which Q212P is selectively processed at the cell surface.

We hypothesized that extracellular PrP release might also reduce the surface PrP levels. To test this hypothesis, we pulse-labeled cells, collected the conditioned media (CM), and examined whether the newly synthesized PrP was recovered from the CM by an RFP-specific antibody. As expected, newly synthesized PrP-RFP, but not free RFP, was selectively recovered from the CM of Q212P cells. Extracellular Q212P proved to be a fully mature form synthesized through the conventional secretory pathway, as revealed by its similarity in gel mobility to the Endo H-resistant surface PrP (of note, Endo H selectively cleaves simple modifications of N-linked glycans processed by ER enzymes) (Fig. 2D) and the inhibition of its secretion by monensin (of note, monensin prevents protein secretion from the medial to trans cisternae of the Golgi complex) (Fig. 2E). Thus, Q212P mutation might be able to catalyzes the extracellular release of surface PrP without affecting endocytosis.

3.3. ADAM10 catalyzes Q212P shedding at the cell surface

We aimed to identify the factor responsible for promoting the extracellular release of surface Q212P and first hypothesized that sheddase ADAM10, a surface metalloproteinase that proteolytically cleaves the ectodomain of surface PrP [21,33] was a promising candidate. This hypothesis was supported by two notable preliminary results. First, surface PrP was shed by N-ethylmaleimide (NEM) (Fig. S3A), a thiol-modifying reagent that is reported to activate sheddase ADAM10 [34]. Second, the extracellular Q212P level was decreased by GI254023X (Fig. S3B), a potent inhibitor of ADAM10 [33].

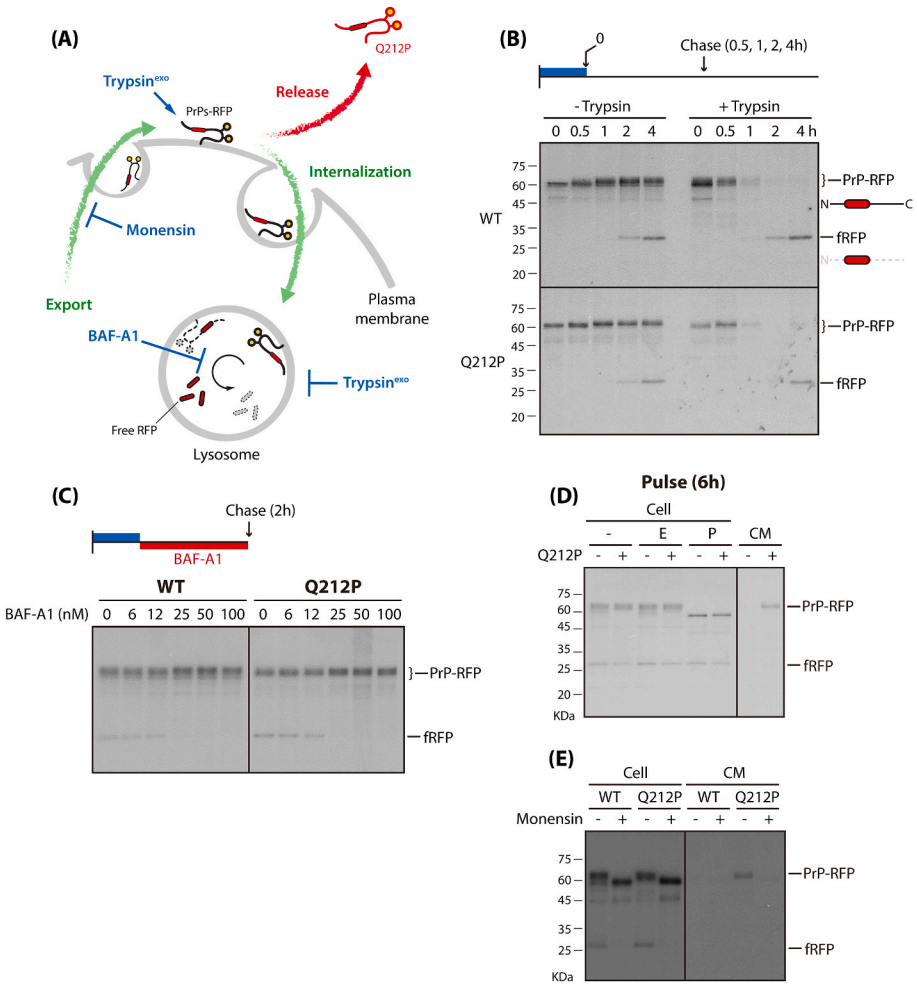

Fig. 2. Analysis of Q212P release into the extracellular space

(A) The lysosome-restricted free RFP generation. The expected metabolism and processing of PrP-RFP were indicated by green arrows; the differential rate in lysosome deliveries were assessed by monitoring the level of free RFP in cells expressing RFP-inserted PrP. Reagents used in this study for determining the localization of PrPs were shown in blue, and the extracellular release of surface Q212P was indicated by the red arrow.

(B) The effect of Q212P mutation on the secretory trafficking of PrP was assessed by the surface-restricted protease digestion. Cells expressing wtPrP-RFP and Q212P-RFP were pulse-labeled for 30 min and followed by the chase as described in the protocol (upper panel). At the indicated time points, intact radioactive cells were incubated for 10 min in the absence (- Trypsin) or presence (+Trypsin) of exogenously added trypsin (0.25%). Fully solubilized cells were diluted 10-fold with IPT buffer and subjected to immunoprecipitation with an RFP-specific antibody (1:500). Note, fRFP: free RFP resistant to lysosomal acidic protease.

(C) The effect of Q212P mutation on the lysosome-restricted free RFP generation was validated by lysosome inhibition. Pulse-labeled cells expressing wtPrP-RFP and Q212P-RFP as in (B) were chased for 2 h in the absence and presence of bafilomycin-A1 (BAF-A1) at the indicated amount. The radioactive cells were fully solubilized and subjected to immunoprecipitation with an RFP-specific antibody.

(D) The effect of Q212P mutation on the extracellular release of surface PrP was confirmed by the detection of fully glycosylated PrP in the CM. Cells expressing wtPrP-RFP and Q212P-RFP were pulse-labeled in methionine-free and cysteine-free DMEM supplemented with 10% dialyzed FBS, 0.6 μM methionine, and 2 μM cysteine for 6 h. The fully solubilized cells were diluted, digested with Endo H or PNGase F, and subjected to immunoprecipitation with an RFP-specific antibody. Extracellular PrP-RFP was also captured by an RFP-specific antibody in a similar manner. Note, CM; conditioned media, E: Endo H, P: PNGase F.

(E) Q212P matured through the conventional secretory pathway before extracellular release. The indicated pulse-labeled cells were further incubated in complete media in the absence or presence of monensin (10 μM) for 4 h. The fully solubilized cells and cell culture media (CM) were subjected to immunoprecipitation with an RFP-specific antibody as in (D). (For interpretation of the references to colour in this figure legend, the reader is referred to the Web version of this article.)

To obtain more direct evidence, we established an ADAM10-disrupted (ΔADAM10) cell line using the CRISPR/Cas9-mediated gene editing. Defective gene expression and protein elimination of ADAM10 were confirmed by RT-PCR and immunoblotting, respectively (Fig. 3A). This cell line was further engineered with inducible expression of stably integrated Q212P-RFP. We monitored the newly synthesized Q212P-RFP recovered in the cell lysates or the CM to determine whether ADAM10 was required for the steady-state shedding of Q212P. Comparative analysis of extracellular Q212P-RFP newly synthesized from pulse-labeled wild-type (WT) and ΔADAM10 cells showed a clear inhibition of Q212P shedding in ΔADAM10 cells (Fig. 3B, left panel, see also Fig. 4C). This inhibitory Q212P shedding conferred an increase in the level of surface Q212P but was not reversed by NEM (Fig. 3B, right panel, see also Fig. 4C). In contrast, the general pattern of free RFP generation was changed neither by ΔADAM10 alone nor in combination with NEM (Fig. 3B), consistently suggesting that ADAM10 was not functionally involved in Q212P endocytosis (Fig. 2B, see also Fig. S2A). In this context, NEM-induced PrP shedding differed from the steady-state Q212P shedding in two notable aspects. First, it was not specific for Q212P, and second, it inhibits PrP endocytosis as judged by the decreased level of free RFP during the chase.

Moreover, the sheddase activity of ADAM10 for Q212P appeared to be exerted at the cell surface. This was revealed by the inducible re-expressions of wt and mutant (i.e., CXXC-to-AXXA substitution) ADAM10 in ΔADAM10 cells. Q212P shedding was restored by the re-expression of wtADAM10, but not by that of the mutant ADAM10 (Fig. 3C) previously shown not to be expressed on the cell surface by being converted into the inactive conformation [35,36]. An additional result in line with our biochemical analyses was also observed in cells chased with CHX and verified by direct visualization of Q212P-RFP restored on the cell surface of ΔADAM10 cells (Fig. 3D). Collectively, these observations suggested that the Q212P mutation promoted the

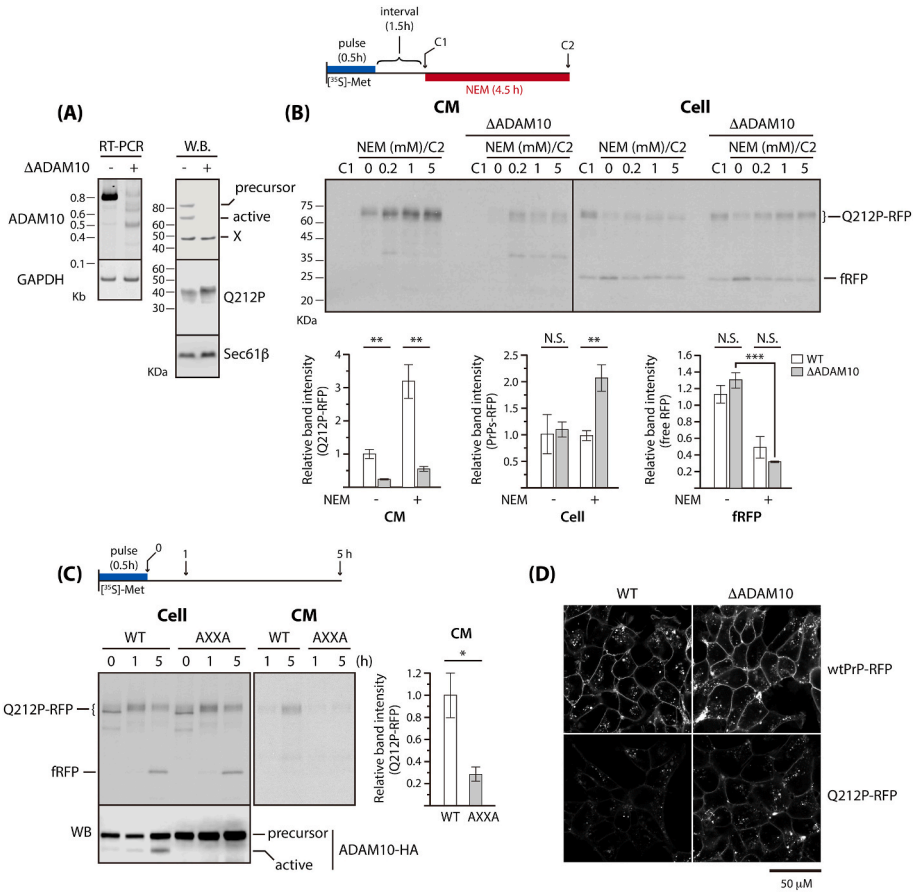

Fig. 3. Analysis of ADAM10-mediated Q212P shedding

(A) ADAM10-deficient cells expressing Q212P-RFP were established using CRISPR/Cas9-mediated genome editing (ΔADAM10) and verified by RT-PCR (left panel) and immunoblotting with ADAM10-specific antibody (right panel). Note, X: non-specific band

(B) The effect of ADAM10 on Q212P shedding was analyzed by pulse-chase experiments. Wild type (WT) and ΔADAM10 cells expressing Q212P-RFP were pulse-labeled for 30 min and allowed to recover for 1.5 h ("C1"), followed by the chase for an additional 4.5 h ("C2") in the absence or presence of NEM as indicated. The fully solubilized cells and CM were subjected to immunoprecipitation with an RFP-specific antibody. Plotted are the changes of intact Q212P-RFP (left panel) and free RFPs (middle panel) in cells and CMs (right panel) by NEM (5 mM) treatment ($n = 3$), and significance was considered with p-values as described in "Materials and Methods". Note, "N·S." means "Not Significant"

(C) The importance of surface expression of ADAM10 in Q212P shedding was analyzed. ΔADAM10 cells expressing Q212P-RFP were transfected with constructs expressing wild-type or mutant (AXXA) ADAM10 fused with HA epitope and subjected to pulse-chase experiments as described in the upper panel. At the indicated time points, the cells and CM were harvested and immunoprecipitated with an RFP-specific antibody (1:500). The expression of transfected ADAM10 was detected in the fully solubilized cells by immunoblotting with an anti-HA antibody (1:5000). The plots represent the relative amount of Q212P-RFP in the CM of cells expressing wild-type versus mutant ADAM10 harvested at 5 h after the chase was plotted ($n = 3$; $p = 0.017$)

(D) Surface expression of wtPrP-RFP and Q212P-RFP was visualized by direct RFP fluorescence in wild-type and ΔADAM10 cells following treatment with cycloheximide (100 μg/mL) for 1 h. Scale bar: 50 μm.

extracellular shedding of PrP via ADAM10 at the cell surface.

3.4. Surface Q212P catalytically interacts with ADAM10

Given the catalytic activity of ADAM10 on Q212P shedding, we inferred that ADAM10 discriminated Q212P mutation through direct interaction. To this end, we created stable cell lines expressing PrPs inserted by GFP (PrPs-GFP). In the preliminary experiment, we subjected these cell lines to a conventional co-IP and examined the interaction of PrPs with endogenous ADAM10. The cells used in this study synthesized two different endogenous ADAM10 corresponding to the intracellular and surface forms whose pro-domains were uncleaved and cleaved by proprotein convertases, furin and PC7, respectively [37,38]. Of these two forms, the intracellular form (i.e., the precursor form) was observed to interact selectively with Q212P, suggesting that misfolded Q212P may be escorted by ADAM10 while passing through the secretory pathway [19]. In contrast, the surface form appeared to interact with neither wtPrP nor Q212P (Fig. S4A). This may be attributed to the Q212P shedding is mediated by a rapid enzymatic reaction resulting from its transient interaction with ADAM10.

This technical problem could be solved by stabilization of the interaction using DSP, a reversible crosslinker, followed by surface-restriction labeling with an FLAG-conjugated GFP-Nb (FLAG-Nb). Using this method, the surface protein complexes containing PrPs-GFP were labeled selectively with Nb, recovered successfully by anti-FLAG antibody (Fig. S4B), and analyzed by immunoblotting with ADAM10-specific antibody (Fig. 4A). Given that ADAM10-mediated PrP shedding occurred at the cell surface (Fig. 3C), surface ADAM10 (i.e., active form lacking pro-domain) was crosslinked with both wtPrP and Q212P and successfully recovered by Nb. However, the amount of ADAM10 recovered with Q212P was noticeably less than that with wtPrP. This could be attributed to the rapid extracellular release of cleaved Q212P (Fig. 4B). In contrast, ADAM17 (Fig. S4C), the structural and functional homolog of ADAM10, was observed not to interact with Q212P or wtPrP (Fig. 4B) and did not appear to be involved in Q212P shedding (Fig. 4C, see also Fig. S4D), indicating that PrP is not the substrate of ADAM17. This was shown by pulse-chase experiments in ΔADAM17 cells in the presence and absence of NEM (Fig. 4C, see also Fig. S4D). Given the model of ADAM10-mediated Notch proteolysis to be discussed later [39], we hypothesized that ADAM10 activity could be catalyzed by the interaction with Q212P, in a manner similar to NEM, but not by wtPrP.

3.5. Q212P shedding is redox-sensitive

Early nuclear magnetic resonance (NMR) structures and X-ray absorption measurements highlighted a unique feature in the secondary structure of Q212P distinctive to that of wtPrP [40,41]. They revealed that its C-terminal region was readily convertible from its native to a pathogenic form. However, we failed to identify any noticeable difference in the two typical determinants indicating PrP proteotoxicity, detergent solubility, and protease sensitivity between wtPrP and Q212P under normal conditions and in ΔADAM10 (Fig. S5A). Instead, unlike wtPrP, newly synthesized Q212P appeared to be sensitive to

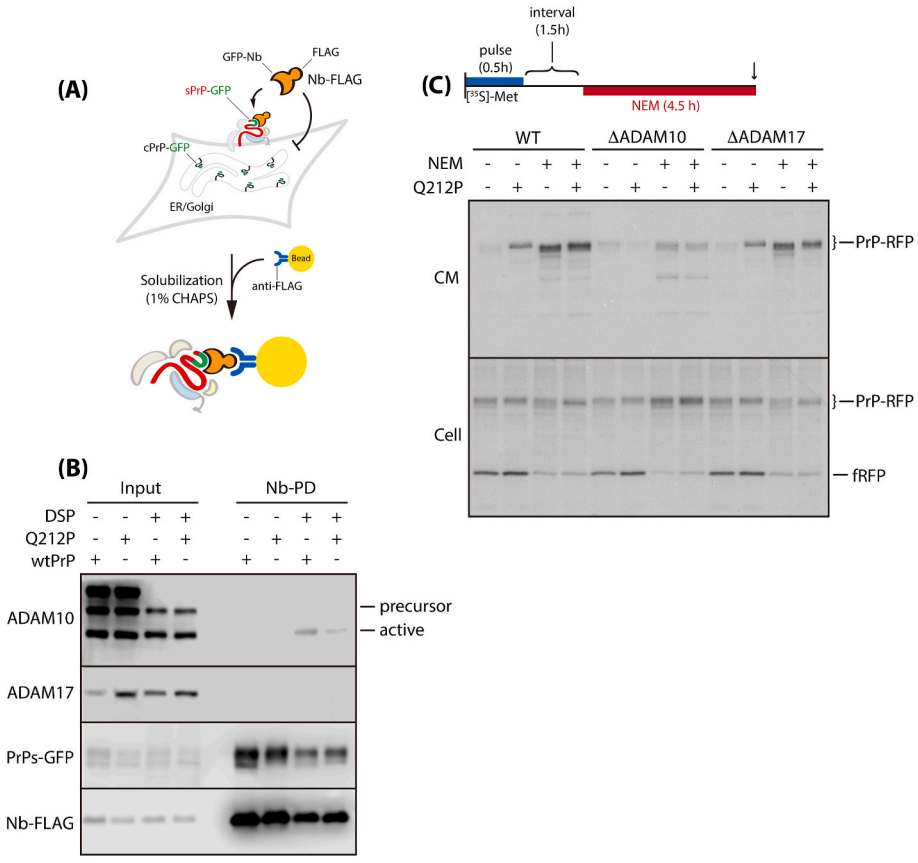

Fig. 4. Analysis of catalytic interaction between ADAM10 and Q212P

(A) Experimental strategy of surface-restricted Nb labeling to confirm the dynamic interactions between ADAM10 and PrPs is described.

(B) Surface interaction of PrPs and ADAM10 was assessed by the surface-restricted Nb labeling as in (A). Cells expressing wtPrP and Q212P (PrPs) inserted by GFP were crosslinked with DSP (2 mM). Complexes containing PrPs-GFP labeled with Nb were recovered by immobilized anti-FLAG antibody (Nb-PD), eluted by FLAG peptides (1 mg/mL), and analyzed by immunoblotting with ADAM10 (1:1000), ADAM17 (1:1000), GFP (1:2000), and FLAG (1:1000)-specific antibodies.

(C) Effects of ADAM17 on PrP shedding were analyzed by pulse-chase experiments. WT, ΔADAM10, and ΔADAM17 cells expressing wtPrP-RFP and Q212P-RFP were pulse-labeled for 30 min and allowed to recover for 1.5 h, followed by the chase for an additional 4.5 h in the presence of NEM as in Fig. 3B. The fully solubilized cells and CM were subjected to immunoprecipitation with an RFP-specific antibody (1:500).

(D) The catalytic interaction of ADAM10 with Q212P at the cell surface is described.

environmental redox perturbations and was detected with additional high-molecular-weight smears by DTT (Fig. 5A) previously shown to inhibit intramolecular disulfide bonds within PrP [20]. These bands were found to be SDS-resistant and confirmed to undergo PNGase F-resistant glycan modifications at least in part during passage through the Golgi apparatus (Fig. S5B). Further analysis of the native size on sucrose gradient suggesting the oligomerization propensity of Q212P under redox perturbations suggested the possibility that these bands were early intermediates of oligomeric Q212P (hereafter, referred as "Q212P*") (Fig. 5B). These results collectively suggested that Q212P had an intrinsically vulnerable conformation to the environmental redox perturbations.

We further investigated the effect of DTT on Q212P shedding using the CM analysis. As expected, the newly synthesized Q212P* remained unreleased from the surface of the DTT-treated cells. Upon DTT withdrawal, the Q212P* was reversibly shed from the surface and increased in the CM with a proportional decrease in the surface level (Fig. 5C). Accelerated endocytosis and ER stress were not involved in these reactions, as revealed by the unchanged free-RFP levels and failure to generate Q212P* by an ER stress inducer thapsigargin (Tg), respectively (Fig. S5C). In a similar manner, we analyzed Q212P in the ΔADAM10 cells. Consistent with the observation in the WT cells (Fig. 5C), Q212P* was also observed in ΔADAM10 cells treated with DTT and was more prominent than in WT cells. However, unlike WT cells, the inhibitory shedding of the Q212P* was hardly restored in ΔADAM10 cells, even by DTT withdrawal (Fig. 5D). This finding was a plausible explanation for the increase in Q212P* on the surface of ΔADAM10 cells. The redox-sensitive inhibition of Q212P shedding was, therefore, reversible as long as ADAM10 was active (Fig. 5E).

3.6. *Inhibitory Q212P shedding promotes cell proliferation*

Given that oligomer-prone PrP exacerbated neurotoxicity and neuronal degeneration [42,43], persistent Q212P shedding by uncontrolled ADAM10 activity could eventually be detrimental unless extracellular Q212P was efficiently eliminated by a clearance mechanism. In contrast, inhibitory Q212P shedding might be more favorable to cells as misfolded surface PrP can be endocytosed eventually into lysosomes for degradation. This was validated by the ability of ΔADAM10 to promote colony formation in single cells expressing Q212P (Fig. 6A). Comparable results were also observed in long-term cultures of mixed cells expressing fluorogenic PrPs and verified by the predominant visualization of ΔADAM10 cells expressing Q212P-RFP (Fig. S6). These observations suggested a potential anti-proliferative effect of extracellular Q212P, with our results consistently demonstrating the efficient endocytosis of Q212P despite ΔADAM10 (Fig. 6B). This was hinted by the sequential centrifugation of the CM (Fig. 6C) showing that the extracellular Q212P was mostly insoluble and precipitated by ultracentrifugation at 100,000×*g* (P100) and 200,000×*g* (P200) (Fig. 6D).

Intriguingly, ADAM10 was also detected in the CM. Extracellular ADAM10 was apparently released from the cell surface but appeared to be independent of Q212P shedding for the following reasons. First, this reaction was not Q212P-selective, as evident through the detection of ADAM10 in the CM of wtPrP cells (Fig. 6D-left and Fig. 6D-middle). Second, ADAM10 was recovered predominantly in S200 rather than P200, indicating that, unlike Q212P, it was mostly present in a soluble form (Fig. 6D-middle and Fig. 6D-right). Last, extracellular ADAM10 was the same in size as the surface form (Fig. 6D-left). In addition, we detected Hsp 90, a major cargo contained in the extracellular vesicles (EVs) such as exosomes [44], in the ADAM10-enriched S200 of both wtPrP and Q212P cells (Fig. 6D-right). This result was in agreement with a previous report suggesting that ADAM10 is incorporated into EVs and spontaneously secreted [45].

Besides Q212P and ADAM10, two small fragments were additionally detected in S200 by an RFP-specific antibody (Fig. 6D-right). Considering that RFP was inserted into the N-terminal region of PrP, these

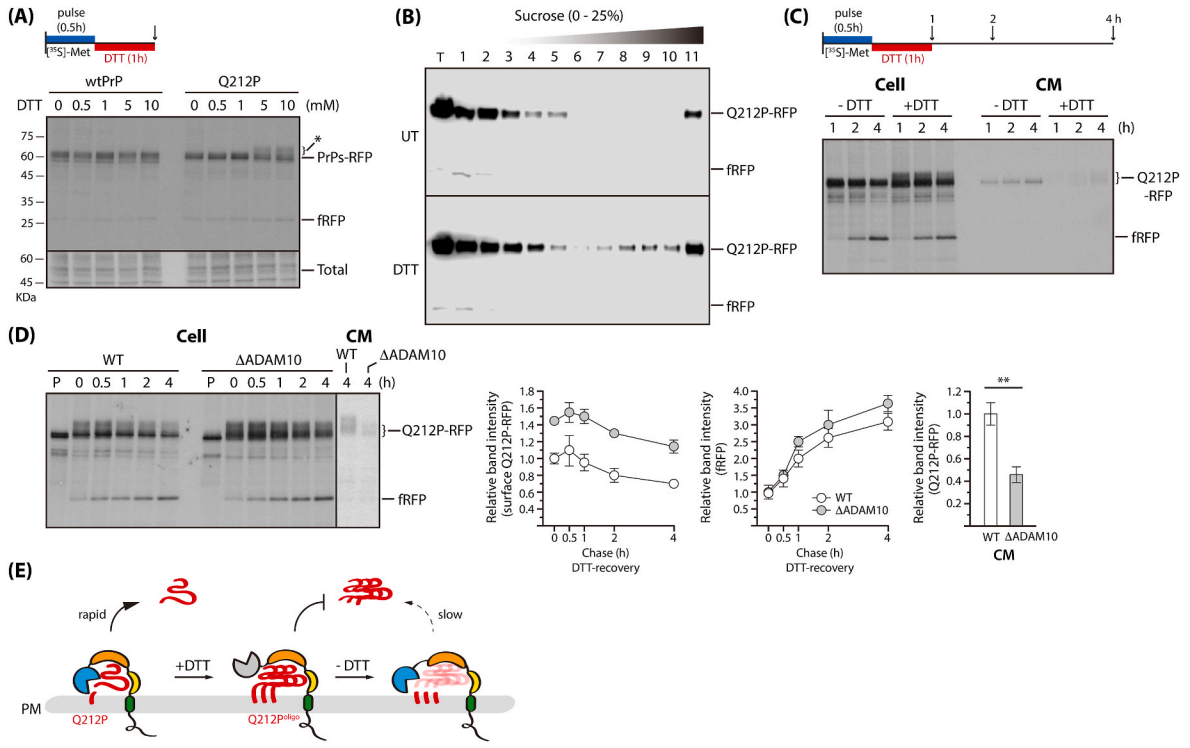

Fig. 5. Analysis of redox-sensitive Q212P shedding

(A) Q212P* synthesis induced by DTT was analyzed by pulse-chase experiments. Cells expressing wtPrP-RFP and Q212P-RFP were pulse-labeled followed by the chase for 1 h in the absence or presence of DTT as indicated. The fully solubilized cells were subjected to immunoprecipitation with an RFP-specific antibody. Equal loading was confirmed by the detection of total proteins newly synthesized. Note, *: Q212P*

(B) A higher oligomerization propensity of Q212P* was analyzed by the density gradient centrifugation. Cells expressing Q212P-RFP were treated with DTT (10 mM) for 1 h, solubilized in IP buffer containing 1% CHAPS, and separated on the sucrose gradient (5–25%) for 3 h in TLS-55 rotor at 50,000 rpm. Each fraction from the top to the bottom of the sucrose gradient was blotted with an RFP-specific antibody (1:5000). Note, T: unfractionated protein samples (0.1 vol)

(C) Q212P* shedding was analyzed by pulse-chase experiments. Cells expressing Q212P-RFP were pulse-labeled for 30 min, chased in the absence ("-DTT") or presence of DTT (10 mM) ("+DTT") for 1 h, and recovered for the indicated time after DTT withdrawal (upper panel). Cells were fully solubilized and subjected to immunoprecipitation with an RFP-specific antibody

(D) The effect of ADAM10 on Q212P* shedding was determined in ΔADAM10 cells in the same method as described in **(C)**. The plots represent the changes of surface Q212P-RFP (left panel) and free RFPs in cells (middle panel) and CMs (right panel) by ADAM10 depletion ($n = 3$). The significance was analyzed through p-values calculated using the student's-t test as described in "Materials and Methods".

(E) Redox-sensitive Q212P shedding is described.

fragments were most likely those of the N-terminal PrP (i.e., N1) proteolytically processed by various proteases and liberated from the cell surface in soluble form. Even though one such typical protease responsible for this cleavage (i.e., α-cleavage) is ADAM10 [46,47], N1 fragments were still produced in ΔADAM10 cells (Fig. 6E). Therefore, ADAM10 was more actively involved in ectodomain shedding near the site of GPI-anchor addition in the C-terminus than α-cleavage within the central hydrophobic region of PrP.

4. Discussion

In this study, we illustrated mutant-selective extracellular release of surface PrP by showing spatiotemporal differences in the metabolism and processing of PrP attributed to the catalytic activity of sheddase ADAM10. The new findings are twofold. One is the discovery of a disease-causing human mutation (Q212P) that promoted ectodomain shedding of surface PrP. The other is the molecular basis for the susceptibility of ADAM10-mediated Q212P shedding to environmental redox perturbations. Our intensive biochemical analysis combined with mutational analyses provided clues to several unresolved issues related to the peripheral pmQC aimed to remove ERAD-resistant misfolded GPI-anchored PrP (Fig. 7).

4.1. Steps susceptible to Q212P mutation during the PrP metabolism

pmQC is a regulated process that limits the endocytic flux of misfolded PrP into lysosomes from the cell surface for degradation. This endocytosis is beneficial to cells as it reduces the burden of lysosomes owing to the misfolded PrP, therefore ensuring the safety of the endocytic pathway [20]. However, the physiologically relevance of this regulation was questionable, as all studies were focused on artificial mutants lacking one or both cysteine residues within PrP [18,20]. Therefore, we aimed to identify pmQC clients from ~30 disease-causing PrP mutants that are reported to metabolize and process differently than wtPrP [14,32]. We, for the first time, reported the Q212P mutation that selectively increases fully glycosylated PrP.

There are various possible reasons for the relative increase in fully glycosylated Q212P (Fig. 1A). First, glycosylation-defective subpopulations might be degraded by ERAD [4]. However, this is least likely because PrP is synthesized with covalent attachment to the ER membrane via a GPI-anchor and poorly degraded by ERAD [10]. Second, the Q212 mutation might inhibit the endocytosis of misfolded PrP from the cell surface into the lysosome for degradation [20]. This did not appear to be the principal reason because the Q212P mutation did not interfere with lysosome-restricted free RFP generation in our analyses (Fig. 2B). Third, the Q212P mutation might enhance the rate of PrP transport to ensure the safety of compartments involved in the secretory

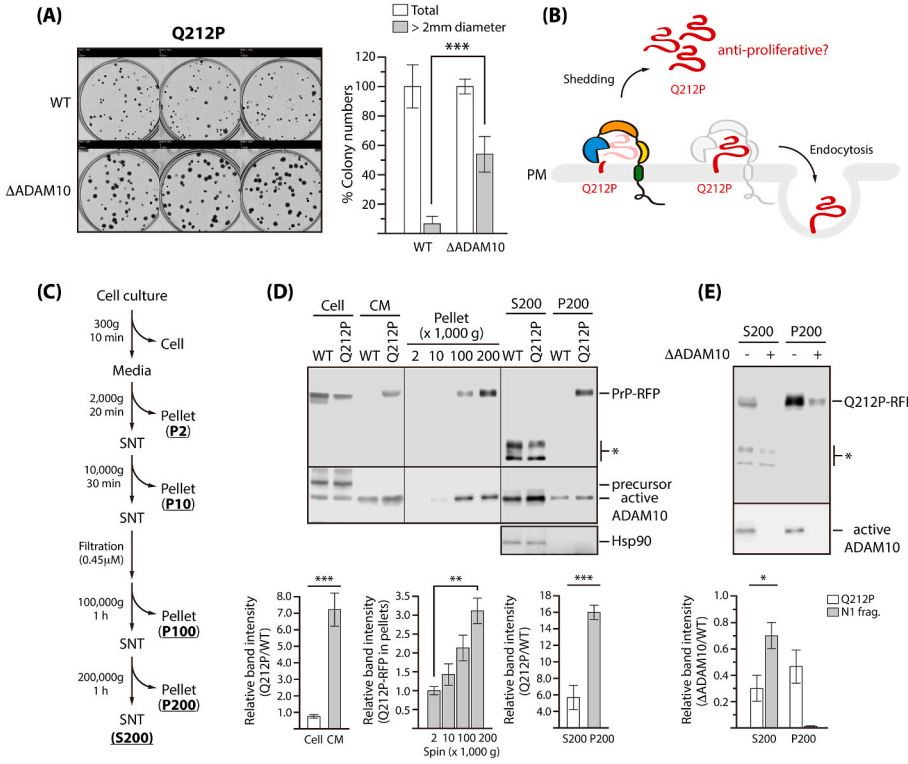

Fig. 6. Analysis of the proliferation-promoting effect of inhibitory Q212P shedding

(A) The effect of inhibitory Q212P shedding on cell proliferation was determined by the colony-forming assay. Wild-type and ADAM10-deficient (ΔADAM10) cells expressing Q212P-RFP were cultured for 3 weeks in the presence of Dox, and allowed to form colonies, that were visualized by staining with crystal violet (left panel). The relative number of large colonies (>2 mm diameter) out of total colonies from three independent experiments (three times in an independent experiment) are plotted as a percentage, and significance was considered with *p*-values (left panel).

(B) The potential proliferation-promoting effect of inhibitory Q212P shedding is illustrated

(C) The protocol shows the sequential centrifugation of CMs containing wtPrP-RFP and Q212P-RFP.

(D) The solubility of extracellular Q212P was examined by sequential centrifugation. Cells expressing wtPrP-RFP and Q212P-RFP were induced by Dox treatment for 24 h and subjected to centrifugal fractionation as described in (C). PrPs-RFP concentrated in indicated fractions were detected by immunoblotting with an RFP-specific antibody. The plots represent the changes of surface and extracellular Q212P-RFP in indicated fractions by ADAM10 depletion ($n = 3$), and significance was considered with *p*-values as described in "Materials and Methods".

(E) CMs of wild-type and ΔADAM10 cells expressing Q212P-RFP were centrifuged at 200,000×*g* for 1 h. The supernatant (S200) and pellet (P200) were subjected to immunoblotting with an RFP-specific antibody. The plots represent the changes of Q212P and N1 fragments in CMs by ADAM10 depletion ($n = 3$).

(For interpretation of the references to colour in this figure legend, the reader is referred to the Web version of this article.)

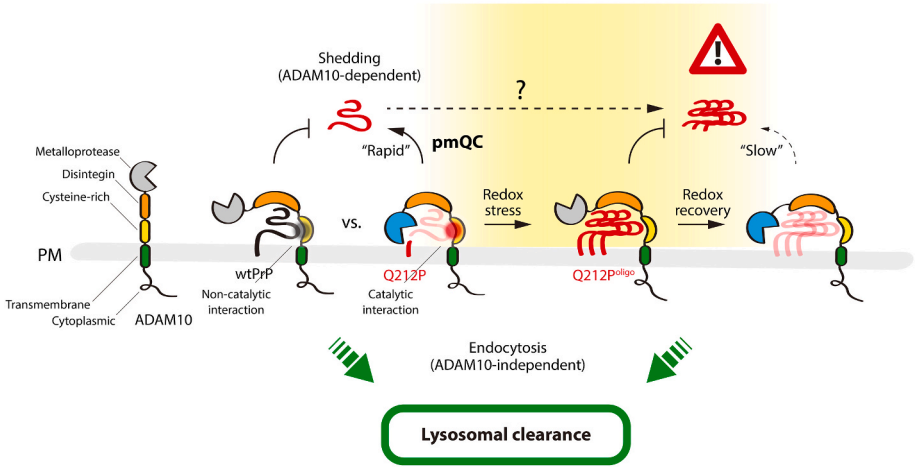

Fig. 7. A working model depicting the role of ADAM10 in promoting Q212P shedding

On the cell surface, the PrP can interact with the cysteine-rich region of ADAM10, either catalytically or non-catalytically. Q212P mutation provides catalytic interaction of PrP with ADAM10, switching the conformation of the cysteine-rich region, allowing PrP to access the ADAM10 active site, and inducing its extracellular shedding. Under redox perturbation, inhibitory Q212P shedding induces the surface accumulation of oligomeric Q212P but is restored, albeit somewhat slowly, upon redox recovery as long as ADAM10 is activated. Nevertheless, cells prefer ADAM10-independent endo-lysosomal degradation to eliminate surface Q212P because it is more efficient than ADAM10-dependent extracellular shedding. This strategy renders cells more capable of fully digesting misfolded surface Q212P that may exert unexpected protein toxicity when released into the extracellular space.

pathway [18,19]. This was validated by the accelerated complex glycan modifications of Q212P compared to that of wtPrP in the pulse-chase analyses (Fig. 1C). Last, the Q212P mutation possibly inhibited the release of surface PrP into the extracellular space. Unexpectedly, the extracellular release of newly synthesized PrP was rather triggered by the Q212P mutation but was insufficient to completely remove the misfolded PrP from the cell surface (Fig. 2). These explanations allowed us to conclude that the rate of secretory trafficking (i.e., RESET) and extracellular release (i.e., pmQC) determine the surface level of pathogenic Q212P, as further discussed in Supplementary Note.

4.2. *Effect of modulation of ADAM10 activity on Q212P shedding*

Given the fact that the Q212P mutation promotes PrP shedding, we inferred that ADAM10 would interact with Q212P at the cell surface with a higher affinity than with wtPrP. However, their transient interaction on the cell surface posed a major challenge to validating this idea. Our attempt to stabilize the cell-surface interaction was able to successfully detect ADAM10 bound to PrP, but this interaction was apparently attenuated by the Q212P mutation. A logical situation supporting this observation would be a rapid release of surface Q212P from the cell surface immediately after the transient catalytic interaction with

ADAM10. This may be key to the molecular basis of mutant-selective PrP shedding, as supported by the facts suggested in previous studies as follows.

First, it is possible that the conformation of ADAM10 is switched from the resting state to the active state mediated by its interaction with Q212P. This idea was suggested by the model of ADAM10-mediated Notch proteolysis derived from the X-ray crystal structure of the mature ADAM10 ectodomain [39]. Most notably, the ADAM10 catalytic site adopts a closed and autoinhibited conformation in the resting state. At this stage, the metalloproteinase domain is partially closed by an intramolecular cysteine-rich domain, limiting the access to the active site. In contrast, upon ligand binding, the activated Notch receptor opens and directly contacts the ADAM10 catalytic site to promote cleavage. Substrate selectivity is, therefore, not only a cause of a typical interaction of the substrate and ADAM10 but also the conformation of the substrate-binding pocket of ADAM10 [48,49]. Likewise, the Q212P mutation may indicate an open conformation of this pocket, which is compatible with a potential mechanism of the mutant-selective PrP shedding of ADAM10.

Second, disulfide exchange switches the conformation of the cysteine-rich region and modulates substrate access to the ADAM10 active site, governing the catalytic activity and substrate selectivity of ADAM10. This has been previously proven by the conformation-specific antibody 8C7, which binds to a conformationally active cysteine-rich domain and inhibits dynamic shuffling of the disulfide linkage with a thioredoxin CXXC motif [35,50,51]. As predicted from the structure, inhibitory disulfide shuffling keeps the ADAM10 active site open and enhances its catalytic activity on the substrate, for example, inhibiting Notch activity [35,39]. In our study, for PrP, comparable results were observed by the exposure to the thiol-modifying reagent NEM, which inhibited dynamic rearrangement of disulfide exchanges; however, in contrast to the steady state, wtPrP was also shed at a similar efficiency to Q212P (Fig. S3A). Although the structural basis for the opening of the ADAM10 active site by the Q212P mutation remains unsolved, our biochemical analyses allowed us to speculate that, similar to the actions of 8C7 and NEM, the Q212P mutation inhibited disulfide exchange in the cysteine-rich region, relieved ADAM10 autoinhibition, and catalyzed ADAM10 activity for PrP shedding.

Last, Q212P shedding is also likely to be also regulated by tetraspanins (Tspans) that form microdomains where ADAM10 is predominantly localized [52–54]. There are 33 reported human Tspans (i.e., Tspan1-Tspan33) that interact with membrane proteins including cell adhesion, signaling molecules, and proteolytic sheddase such as ADAM10 to regulate their intracellular trafficking, lateral mobility, and cell surface clustering [52,55]. Unlike the other Tspans, the TspanC8 subgroup (TspanC8s) has eight cysteine residues within the main extracellular region, which form structurally important disulfide bridges for inter-Tspan interactions and regulate ADAM10 activity [56–58]. The subgroup consists of six members (i.e., Tspan5, Tspan10, Tspan14, Tspan15, Tspan17, and Tspan33) and forms six different "scissor complexes" with ADAM10 that have distinct substrate repertoires [59,60]. One such notable member of TspanC8s is Tspan15 which has been identified to interact with ADAM10 and suggested as a potent regulator of ADAM10 proteolytic activity [61]. More recently, inhibitory PrP shedding has been observed in Tspan15 knockout mice [62], suggesting the possibility that Tspan15 causes ADAM10 to release PrP from the cell surface. Although there is currently no definitive evidence to address the dynamic assembly and disassembly of the Tspan15-ADAM10-Q212P complex in Tspan microdomain, it is likely that Tspan15 and/or possibly the other members of TspanC8s modulate ADAM10-mediated Q212P shedding in the complex.

4.3. Importance of regulation in cell and organism

Given the vulnerability of Q212P to environmental redox perturbations, catalysis of sheddase ADAM10 appears to be a "double-edged sword" that, on the one hand, protects the cell surface from Q212P, but on the other, spreads misfolded Q212P to neighboring cells [21,22]. These opposing reactions must be fine-tuned via ADAM10 in a timely and cooperative manner, otherwise, Q212P accumulates either on the cell surface or in the extracellular space. Although we did not perform an in-depth investigation on the intrinsic properties of Q212P, our analyses in ΔADAM10 cells provided several valuable clues for a better understanding of the pathological/physiological significance of Q212P shedding mediated by its catalytic interaction with ADAM10.

First, inhibitory Q212P shedding was observed as pro-proliferative. This effect was seen in ΔADAM10 cells expressing Q212P and confirmed by an increase in the size rather than the number of viable colonies grown from single cells (Fig. 6A, see also Fig. S6). In addition, it was not surprising that the cell surface accumulation of Q212P mediated by inhibitory shedding did not induce proteotoxicity, as it was determined to be similar to wtPrP in terms of detergent solubility and protease sensitivity (Fig. S5A), the two typical indicators of proteotoxicity for PrP [14,20]. Upon release, the extracellular Q212P was expected to be deleterious on its own, as shown by its reduced solubility in the CM, but was diluted to ineffective concentration in the extracellular space, therefore, making it difficult to observe overt proteotoxicity. In contrast, while on the cell surface, Q212P only affected surrounding cells, it was rapidly endocytosed into lysosomes for degradation before exerting proteotoxicity. This might be a plausible explanation for the increased size of the viable colonies as a result of inhibitory Q212P shedding (Fig. 6).

Second, ADAM10 served as a negative regulator of pmQC. This fact may be reasonable owing to Q212P's tendency to shed extracellularly in contrast to PrP*, a well-known pmQC substrate that is prone to rapid lysosomal degradation [20]. Nonetheless, both Q212P and PrP* were assumed to be RESET substrates that were rapidly delivered to the cell surface from the stressed ER. During RESET, Q212P formed a complex with precursor ADAM10 (Fig. S4A), while PrP* is known to interact with TMED10 [18,20]. Thus, ADAM10 regulates the Q212P with two sequential functions with the precursor ADAM10 serving as a chaperone that shields misfolded Q212P during the post-ER itinerary [19,63], and mature ADAM10 subsequently acting as a sheddase that mediates the proteolytic release of surface Q212P into the extracellular space [21]. Therefore, it can be concluded that ADAM10 participates throughout the secretory itinerary of Q212P, including RESET and pmQC, and allowed PrP accessing the cell surface via RESET to bypass pmQC and get released into the extracellular space (Fig. 7). From a larger perspective, ADAM10 was worth considering as a proteostasis checkpoint to ensure the safety of the secretory and endocytic pathways from misfolded PrP (discussed further in Supplementary Note).

Last, ADAM10 deserves significant consideration as a valuable therapeutic target for various human diseases. Besides PrP [21,33], more than 100 other substrates, including Notch receptor, APP, and cadherin family, are processed by ADAM10 [23,64]. These substrates are important regulators of cell adhesion and receptor signaling, and their dysregulations are often associated with pathological progression in human diseases, such as brain disorders including Alzheimer's disease, prion disease, fragile X-syndrome, Huntington's disease; cancer including T cell acute lymphoblastic leukemia, glioblastoma, breast cancer, squamous cell carcinoma; and immune disorders including psoriasis, systemic lupus erythematosus, rheumatoid arthritis, *Staphylococcus aureus* infections, chronic liver inflammation, atherosclerosis [65]. The role of ADAM10 substrates in these disease progressions suggests the potential of ADAM10 as a promising therapeutic target. For instance, Alzheimer's disease is characterized by deposition of pathogenic amyloid β peptide (Aβ) derived from amyloid precursor protein (APP), an ADAM10 substrate. ADAM10 activation has been expected to inhibit disease progression in Alzheimer's disease [66]. In addition to promoting ADAM10 activity, the therapeutic strategies aimed towards inhibiting its activity by targeting its active site have been tested in the field of synthetic small molecules. Several hydroxamate inhibitors that

chelate the Zn^{2+} of the ADAM10 active site, including GI254023X, have been screened and developed [67,68]. However, despite their high potential demonstrated through the cell and animal-based experiments, they are frequently withdrawn from clinical trials owing to insufficient selectivity, toxicity, and drug resistance [69]. These side effects may be attributed to the varieties of substrates and expression patterns of ADAM10, necessitating a better understanding of the functional consequences of various substrates shed by ADAM10. This requires intensive investigation of the expression, regulation, localization, and interacting partners of ADAM10 in cell culture and animal models.

Funding

This research was supported by Basic Science Research Program through the National Research Foundation of Korea (NRF) funded by the Ministry of Education (NRF-2021R1I1A2040258) and in part by Asan Institute for Life Sciences (2021IL0001 and 2022IL0009).

Author contributions

S–W.K.: Conceptualization, Experimental design, Data analysis, and Manuscript writing; Y·S.: Experimental investigation and Data analysis; K–S.J., D.L., M.S., and H·Y.: Experimental investigation; and Y·S.: Idea and resource provision and Data analysis.

Declaration of competing interest

The authors declare that no competing interests exist.

Data availability

Data will be made available on request.

Acknowledgements

We thank the members of the ER lab. for insightful discussions and the Confocal Microscope Core facility at the ConveRgence mEDIcine research cenTer (CREDIT), Asan Medical Center, for providing support and instrumentation.

Appendix A. Supplementary data

Supplementary data to this article can be found online at https://doi.org/10.1016/j.redox.2022.102456.

References

[1] D. Balchin, M. Hayer-Hartl, F.U. Hartl, In vivo aspects of protein folding and quality control, Science 353 (6294) (2016), aac4354.
[2] I. Braakman, D.N. Hebert, Protein folding in the endoplasmic reticulum, Cold Spring Harbor Perspect. Biol. 5 (5) (2013), a013201.
[3] Z. Sun, J.L. Brodsky, Protein quality control in the secretory pathway, J. Cell Biol. 218 (10) (2019) 3171–3187.
[4] R.S. Hegde, H.L. Ploegh, Quality and quantity control at the endoplasmic reticulum, Curr. Opin. Cell Biol. 22 (4) (2010) 437–446.
[5] F.U. Hartl, Protein misfolding diseases, Annu. Rev. Biochem. 86 (2017) 21–26.
[6] L.C. Walker, Proteopathic strains and the heterogeneity of neurodegenerative diseases, Annu. Rev. Genet. 50 (2016) 329–346.
[7] P.A. Koenig, H.L. Ploegh, Protein quality control in the endoplasmic reticulum, F1000Prime Rep 6 (2014) 49.
[8] E.M. Quan, Y. Kamiya, D. Kamiya, V. Denic, J. Weibezahn, K. Kato, J.S. Weissman, Defining the glycan destruction signal for endoplasmic reticulum-associated degradation, Mol. Cell 32 (6) (2008) 870–877.
[9] S. Clerc, C. Hirsch, D.M. Oggier, P. Deprez, C. Jakob, T. Sommer, M. Aebi, Htm 1 protein generates the N-glycan signal for glycoprotein degradation in the endoplasmic reticulum, J. Cell Biol. 184 (1) (2009) 159–172.
[10] A. Ashok, R.S. Hegde, Retrotranslocation of prion proteins from the endoplasmic reticulum by preventing GPI signal transamidation, Mol. Biol. Cell 19 (8) (2008) 3463–3476.
[11] S.B. Prusiner, Biology and genetics of prions causing neurodegeneration, Annu. Rev. Genet. 47 (2013) 601–623.
[12] D.W. Colby, S.B. Prusiner, Prions, Cold Spring Harbor Perspect. Biol. 3 (1) (2011), a006833.
[13] L. Bernardi, A.C. Bruni, Mutations in prion protein gene: pathogenic mechanisms in C-terminal vs. N-terminal domain, a review, Int. J. Mol. Sci. 20 (14) (2019).
[14] A. Ashok, R.S. Hegde, Selective processing and metabolism of disease-causing mutant prion proteins, PLoS Pathog. 5 (6) (2009), e1000479.
[15] R. Goold, C. McKinnon, S.J. Tabrizi, Prion degradation pathways: potential for therapeutic intervention, Mol. Cell. Neurosci. 66 (Pt A) (2015) 12–20.
[16] S.W. Kang, N.S. Rane, S.J. Kim, J.L. Garrison, J. Taunton, R.S. Hegde, Substrate-specific translocational attenuation during ER stress defines a pre-emptive quality control pathway, Cell 127 (5) (2006) 999–1013.
[17] Y. Lee, H. Eum, D. Lee, S. Lee, Y. Song, S.W. Kang, Mutant-selective topologic conversion facilitates selective degradation of a pathogenic prion isoform, Cell Death Differ. 27 (1) (2020) 284–296.
[18] P. Satpute-Krishnan, M. Ajinkya, S. Bhat, E. Itakura, R.S. Hegde, J. Lippincott-Schwartz, ER stress-induced clearance of misfolded GPI-anchored proteins via the secretory pathway, Cell 158 (3) (2014) 522–533.
[19] E. Zavodszky, R.S. Hegde, Misfolded GPI-anchored proteins are escorted through the secretory pathway by ER-derived factors, Elife 8 (2019).
[20] D. Lee, S. Lee, Y. Shin, Y. Song, S.W. Kang, Thiol-disulfide status regulates quality control of prion protein at the plasma membrane, Faseb. J. 33 (10) (2019) 11567–11578.
[21] H.C. Altmeppen, J. Prox, S. Krasemann, B. Puig, K. Kruszewski, F. Dohler, C. Bernreuther, A. Hoxha, L. Linsenmeier, B. Sikorska, P.P. Liberski, U. Bartsch, P. Saftig, M. Glatzel, The sheddase ADAM10 is a potent modulator of prion disease, Elife 4 (2015).
[22] H.C. Altmeppen, B. Puig, F. Dohler, D.K. Thurm, C. Falker, S. Krasemann, M. Glatzel, Proteolytic processing of the prion protein in health and disease, Am J Neurodegener Dis 1 (1) (2012) 15–31.
[23] J. Pruessmeyer, A. Ludwig, The good, the bad and the ugly substrates for ADAM10 and ADAM17 in brain pathology, inflammation and cancer, Semin. Cell Dev. Biol. 20 (2) (2009) 164–174.
[24] P. Saftig, K. Reiss, The "A Disintegrin and Metalloproteases" ADAM10 and ADAM17: novel drug targets with therapeutic potential? Eur. J. Cell Biol. 90 (6–7) (2011) 527–535.
[25] B. Vincent, E. Paitel, P. Saftig, Y. Frobert, D. Hartmann, B. De Strooper, J. Grassi, E. Lopez-Perez, F. Checler, The disintegrins ADAM10 and TACE contribute to the constitutive and phorbol ester-regulated normal cleavage of the cellular prion protein, J. Biol. Chem. 276 (41) (2001) 37743–37746.
[26] D.R. Taylor, E.T. Parkin, S.L. Cocklin, J.R. Ault, A.E. Ashcroft, A.J. Turner, N. M. Hooper, Role of ADAMs in the ectodomain shedding and conformational conversion of the prion protein, J. Biol. Chem. 284 (34) (2009) 22590–22600.
[27] E.L. Snapp, G.A. Reinhart, B.A. Bogert, J. Lippincott-Schwartz, R.S. Hegde, The organization of engaged and quiescent translocons in the endoplasmic reticulum of mammalian cells, J. Cell Biol. 164 (7) (2004) 997–1007.
[28] R.D. Fons, B.A. Bogert, R.S. Hegde, Substrate-specific function of the translocon-associated protein complex during translocation across the ER membrane, J. Cell Biol. 160 (4) (2003) 529–539.
[29] S. Stefanovic, R.S. Hegde, Identification of a targeting factor for posttranslational membrane protein insertion into the ER, Cell 128 (6) (2007) 1147–1159.
[30] N.A. Franken, H.M. Rodermond, J. Stap, J. Haveman, C. van Bree, Clonogenic assay of cells in vitro, Nat. Protoc. 1 (5) (2006) 2315–2319.
[31] N.E. Sanjana, O. Shalem, F. Zhang, Improved vectors and genome-wide libraries for CRISPR screening, Nat. Methods 11 (8) (2014) 783–784.
[32] Y. Lee, D. Lee, I. Choi, Y. Song, M.J. Kang, S.W. Kang, Single octapeptide deletion selectively processes a pathogenic prion protein mutant on the cell surface, Biochem. Biophys. Res. Commun. 470 (2) (2016) 263–268.
[33] L. Linsenmeier, B. Mohammadi, S. Wetzel, B. Puig, W.S. Jackson, A. Hartmann, K. Uchiyama, S. Sakaguchi, K. Endres, J. Tatzelt, P. Saftig, M. Glatzel, H. C. Altmeppen, Structural and mechanistic aspects influencing the ADAM10-mediated shedding of the prion protein, Mol. Neurodegener. 13 (1) (2018) 18.
[34] R.K. Andrews, D. Karunakaran, E.E. Gardiner, M.C. Berndt, Platelet receptor proteolysis: a mechanism for downregulating platelet reactivity, Arterioscler. Thromb. Vasc. Biol. 27 (7) (2007) 1511–1520.
[35] L. Atapattu, N. Saha, C. Chheang, M.F. Eissman, K. Xu, M.E. Vail, L. Hii, C. Llerena, Z. Liu, K. Horvay, H.E. Abud, U. Kusebauch, R.L. Moritz, B.S. Ding, Z. Cao, S. Rafii, M. Ernst, A.M. Scott, D.B. Nikolov, M. Lackmann, P.W. Janes, An activated form of ADAM10 is tumor selective and regulates cancer stem-like cells and tumor growth, J. Exp. Med. 213 (9) (2016) 1741–1757.
[36] A. Seifert, S. Dusterhoft, J. Wozniak, C.Z. Koo, M.G. Tomlinson, E. Nuti, A. Rossello, D. Cuffaro, D. Yildiz, A. Ludwig, The metalloproteinase ADAM10 requires its activity to sustain surface expression, Cell. Mol. Life Sci. : CM 78 (2) (2021) 715–732.
[37] A.J. Roebroek, J.W. Creemers, T.A. Ayoubi, W.J. Van de Ven, Furin-mediated proprotein processing activity: involvement of negatively charged amino acid residues in the substrate binding region, Biochimie 76 (3–4) (1994) 210–216.
[38] A. Anders, S. Gilbert, W. Garten, R. Postina, F. Fahrenholz, Regulation of the alpha-secretase ADAM10 by its prodomain and proprotein convertases, Faseb. J. 15 (10) (2001) 1837–1839.
[39] T.C.M. Seegar, L.B. Killingsworth, N. Saha, P.A. Meyer, D. Patra, B. Zimmerman, P. W. Janes, E. Rubinstein, D.B. Nikolov, G. Skiniotis, A.C. Kruse, S.C. Blacklow, Structural basis for regulated proteolysis by the alpha-secretase ADAM10, Cell 171 (7) (2017) 1638–1648 e7.
[40] G. Ilc, G. Giachin, M. Jaremko, L. Jaremko, F. Benetti, J. Plavec, I. Zhukov, G. Legname, NMR structure of the human prion protein with the pathological

Q212P mutation reveals unique structural features, PLoS One 5 (7) (2010), e11715.
[41] P. D'Angelo, S. Della Longa, A. Arcovito, G. Mancini, A. Zitolo, G. Chillemi, G. Giachin, G. Legname, F. Benetti, Effects of the pathological Q212P mutation on human prion protein non-octarepeat copper-binding site, Biochemistry 51 (31) (2012) 6068–6079.
[42] S. Simoneau, H. Rezaei, N. Sales, G. Kaiser-Schulz, M. Lefebvre-Roque, C. Vidal, J. G. Fournier, J. Comte, F. Wopfner, J. Grosclaude, H. Schatzl, C.I. Lasmezas, In vitro and in vivo neurotoxicity of prion protein oligomers, PLoS Pathog. 3 (8) (2007) e125.
[43] M. Shafiq, S. Zafar, N. Younas, A. Noor, B. Puig, H.C. Altmeppen, M. Schmitz, J. Matschke, I. Ferrer, M. Glatzel, I. Zerr, Prion protein oligomers cause neuronal cytoskeletal damage in rapidly progressive Alzheimer's disease, Mol. Neurodegener. 16 (1) (2021) 11.
[44] T. Eguchi, K. Ono, K. Kawata, K. Okamoto, S.K. Calderwood, Regulatory roles of HSP90-rich extracellular vesicles, in: A.A.A. Asea, P. Kaur (Eds.), Heat Shock Protein 90 in Human Diseases and Disorders, Springer International Publishing, Cham, 2019, pp. 3–17.
[45] M.D. Keller, K.L. Ching, F.X. Liang, A. Dhabaria, K. Tam, B.M. Ueberheide, D. Unutmaz, V.J. Torres, K. Cadwell, Decoy exosomes provide protection against bacterial toxins, Nature 579 (7798) (2020) 260–264.
[46] D.A. Harris, M.T. Huber, P. van Dijken, S.L. Shyng, B.T. Chait, R. Wang, Processing of a cellular prion protein: identification of N- and C-terminal cleavage sites, Biochemistry 32 (4) (1993) 1009–1016.
[47] J. Liang, Q. Kong, alpha-Cleavage of cellular prion protein, Prion 6 (5) (2012) 453–460.
[48] K.M. Smith, A. Gaultier, H. Cousin, D. Alfandari, J.M. White, D.W. DeSimone, The cysteine-rich domain regulates ADAM protease function in vivo, J. Cell Biol. 159 (5) (2002) 893–902.
[49] P.W. Janes, N. Saha, W.A. Barton, M.V. Kolev, S.H. Wimmer-Kleikamp, E. Nievergall, C.P. Blobel, J.P. Himanen, M. Lackmann, D.B. Nikolov, Adam meets Eph: an ADAM substrate recognition module acts as a molecular switch for ephrin cleavage in trans, Cell 123 (2) (2005) 291–304.
[50] L. Atapattu, N. Saha, C. Llerena, M.E. Vail, A.M. Scott, D.B. Nikolov, M. Lackmann, P.W. Janes, Antibodies binding the ADAM10 substrate recognition domain inhibit Eph function, J. Cell Sci. 125 (Pt 24) (2012) 6084–6093.
[51] S. Dusterhoft, S. Jung, C.W. Hung, A. Tholey, F.D. Sonnichsen, J. Grotzinger, I. Lorenzen, Membrane-proximal domain of a disintegrin and metalloprotease-17 represents the putative molecular switch of its shedding activity operated by protein-disulfide isomerase, J. Am. Chem. Soc. 135 (15) (2013) 5776–5781.
[52] S. van Deventer, A.B. Arp, A.B. van Spriel, Dynamic plasma membrane organization: a complex symphony, Trends Cell Biol. 31 (2) (2021) 119–129.
[53] J. Saint-Pol, M. Billard, E. Dornier, E. Eschenbrenner, L. Danglot, C. Boucheix, S. Charrin, E. Rubinstein, New insights into the tetraspanin Tspan5 using novel monoclonal antibodies, J. Biol. Chem. 292 (23) (2017) 9551–9566.
[54] C. Arduise, T. Abache, L. Li, M. Billard, A. Chabanon, A. Ludwig, P. Mauduit, C. Boucheix, E. Rubinstein, F. Le Naour, Tetraspanins regulate ADAM10-mediated cleavage of TNF-alpha and epidermal growth factor, J. Immunol. 181 (10) (2008) 7002–7013.
[55] S. Charrin, S. Jouannet, C. Boucheix, E. Rubinstein, Tetraspanins at a glance, J. Cell Sci. 127 (Pt 17) (2014) 3641–3648.
[56] S. Charrin, F. le Naour, O. Silvie, P.E. Milhiet, C. Boucheix, E. Rubinstein, Lateral organization of membrane proteins: tetraspanins spin their web, Biochem. J. 420 (2) (2009) 133–154.
[57] D. Xu, C. Sharma, M.E. Hemler, Tetraspanin 12 regulates ADAM10-dependent cleavage of amyloid precursor protein, Faseb. J. 23 (11) (2009) 3674–3681.
[58] O.V. Kovalenko, X. Yang, T.V. Kolesnikova, M.E. Hemler, Evidence for specific tetraspanin homodimers: inhibition of palmitoylation makes cysteine residues available for cross-linking, Biochem. J. 377 (Pt 2) (2004) 407–417.
[59] S. Jouannet, J. Saint-Pol, L. Fernandez, V. Nguyen, S. Charrin, C. Boucheix, C. Brou, P.E. Milhiet, E. Rubinstein, TspanC8 tetraspanins differentially regulate the cleavage of ADAM10 substrates, Notch activation and ADAM10 membrane compartmentalization, Cell. Mol. Life Sci. : CM 73 (9) (2016) 1895–1915.
[60] A.L. Matthews, J. Szyroka, R. Collier, P.J. Noy, M.G. Tomlinson, Scissor sisters: regulation of ADAM10 by the TspanC8 tetraspanins, Biochem. Soc. Trans. 45 (3) (2017) 719–730.
[61] J. Prox, M. Willenbrock, S. Weber, T. Lehmann, D. Schmidt-Arras, R. Schwanbeck, P. Saftig, M. Schwake, Tetraspanin 15 regulates cellular trafficking and activity of the ectodomain sheddase ADAM10, Cell. Mol. Life Sci. : CM 69 (17) (2012) 2919–2932.
[62] L. Seipold, H. Altmeppen, T. Koudelka, A. Tholey, P. Kasparek, R. Sedlacek, M. Schweizer, J. Bar, M. Mikhaylova, M. Glatzel, P. Saftig, In vivo regulation of the A disintegrin and metalloproteinase 10 (ADAM10) by the tetraspanin 15, Cell. Mol. Life Sci. : CM 75 (17) (2018) 3251–3267.
[63] J. Suh, S.H. Choi, D.M. Romano, M.A. Gannon, A.N. Lesinski, D.Y. Kim, R.E. Tanzi, ADAM10 missense mutations potentiate beta-amyloid accumulation by impairing prodomain chaperone function, Neuron 80 (2) (2013) 385–401.
[64] P.H. Kuhn, A.V. Colombo, B. Schusser, D. Dreymueller, S. Wetzel, U. Schepers, J. Herber, A. Ludwig, E. Kremmer, D. Montag, U. Muller, M. Schweizer, P. Saftig, S. Brase, S.F. Lichtenthaler, Systematic substrate identification indicates a central role for the metalloprotease ADAM10 in axon targeting and synapse function, Elife 5 (2016).
[65] S. Wetzel, L. Seipold, P. Saftig, The metalloproteinase ADAM10: a useful therapeutic target? Biochim. Biophys. Acta Mol. Cell Res. 1864 (11 Pt B) (2017) 2071–2081.
[66] R. Postina, A. Schroeder, I. Dewachter, J. Bohl, U. Schmitt, E. Kojro, C. Prinzen, K. Endres, C. Hiemke, M. Blessing, P. Flamez, A. Dequenne, E. Godaux, F. van Leuven, F. Fahrenholz, A disintegrin-metalloproteinase prevents amyloid plaque formation and hippocampal defects in an Alzheimer disease mouse model, J. Clin. Invest. 113 (10) (2004) 1456–1464.
[67] A. Ludwig, C. Hundhausen, M.H. Lambert, N. Broadway, R.C. Andrews, D. M. Bickett, M.A. Leesnitzer, J.D. Becherer, Metalloproteinase inhibitors for the disintegrin-like metalloproteinases ADAM10 and ADAM17 that differentially block constitutive and phorbol ester-inducible shedding of cell surface molecules, Comb. Chem. High Throughput Screen. 8 (2) (2005) 161–171.
[68] M.R. Zocchi, C. Camodeca, E. Nuti, A. Rossello, R. Vene, F. Tosetti, I. Dapino, D. Costa, A. Musso, A. Poggi, ADAM10 new selective inhibitors reduce NKG2D ligand release sensitizing Hodgkin lymphoma cells to NKG2D-mediated killing, OncoImmunology 5 (5) (2016), e1123367.
[69] M.J. Duffy, M. Mullooly, N. O'Donovan, S. Sukor, J. Crown, A. Pierce, P. M. McGowan, The ADAMs family of proteases: new biomarkers and therapeutic targets for cancer? Clin. Proteonomics 8 (1) (2011) 9.